Zygote **24** (December), pp. 900–908. © Cambridge University Press 2016
doi:10.1017/S096719941600023X First Published Online 13 October 2016

Combination of spindle and first polar body chromosome images for the enhanced prediction of developmental potency of mouse metaphase II oocytes

Yukou Sugano[2], *Manami Yazawa*[2], *Sachio Takino*[2], *Sueo Niimura*[2] *and Hideaki Yamashiro*[1]
Laboratory of Animal Reproduction, Graduate School of Science and Technology, Niigata University, Nishiku, Niigata, Japan

Date submitted: 13.03.2016. Date revised: 16.06.2016. Date accepted: 20.07.2016

Summary

The objective of this study was to classify spindle and first polar body (PB1) chromosome images in ovulated mouse oocytes over time to predict the developmental competence of metaphase II (MII) oocytes. Oocytes were collected at 12, 15, 20, and 25 h after human chorionic gonadotropin (hCG) injection, and stained for spindle tubulin, chromosomes, and PB1 chromosomes. MII spindle morphology was classified as tapered type or barrel type and PB1 chromosomes were categorized as aggregated, separated, dot, or collapsed. To determine whether differences in spindle and PB1 images in MII oocytes are associated with fertilization success, we performed *in vitro* fertilization (IVF) at various times after hCG injection. Barrel-type spindles and aggregate-type PB1 were dominant at 12 h after hCG injection. Oocyte spindles collected 1 h after injection were tapered, and PB1 chromosomes were separated. At 20 and 25 h after treatment, spindle and PB1 images were classified as collapsed. The rate of development to 2-cell embryos after IVF did not differ between the 12 h and 15 h treatments; however, it was significantly lower for the 25 h treatment than for other treatments. The rates of development to blastocysts at 12, 15, 20, and 25 h after hCG injection were 61, 46, 42, and 9%, respectively. MII oocytes with barrel-type spindles and aggregate-type PB1 had high rates of fertilization and blastocyst development, and spindle and PB1 characteristics were correlated with the outcomes of IVF and embryo culture. These results suggested that images of spindles combined with those of PB1 chromosomes enable the prediction of oocytic and/or embryonic quality.

Keywords: Developmental rate, First polar body, IVF, Metaphase II, Spindle

Introduction

Preimplantation genetic diagnosis (PGD) is most frequently performed by embryo biopsy in assisted reproductive technology (ART) to detect chromosome aneuploidy owing to advancing maternal age or structural chromosome rearrangements (Stern, 2014). Molecular technologies for aneuploidy testing, including array comparative genomic hybridization (array-CGH), single nucleotide polymorphism arrays, quantitative polymerase chain reaction (PCR), and, most recently, next-generation sequencing-based protocols are used for PGD. Discussion on the cost and scientific, ethical, legal, and social issues surrounding the use of sequence data obtained from embryo biopsies has been initiated, and must continue to avoid eugenic or inappropriate applications of these technologies.

The spindle plays an important role in the normal placement and separation of chromosomes when oocytes undergo meiosis. They are constructed by microtubules, in which α-tubulin and β-tubulin dimers gather (Uchiyama *et al.*, 2008). Spindles congregate at the centre of oocytes in metaphase

[1]All correspondence to: Hideaki Yamashiro. Laboratory of Animal Reproduction, Graduate School of Science and Technology, Niigata University, 2–8050 Ikarashi, Nishiku, Niigata 950–2181, Japan. Tel:/Fax: +81 25 262 6596. E-mail: hyamashiro@agr.niigata-u.ac.jp
[2]Laboratory of Animal Reproduction, Graduate School of Science and Technology, Niigata University, 2–8050 Ikarashi, Nishiku, Niigata 950–2181, Japan.

I (MI) and move to the nearest region in the oolemma of oocytes. The chromosome separates at anaphase I (AI), and the spindle becomes parallel to the oolemma. The spindle turns and becomes perpendicular to the oolemma. Next, the release of the chromosomal halves to the first polar body (PB1) is promoted (Fabritius *et al.*, 2011). It is widely held that defects in metaphase II (MII) spindle morphology and chromosomal alignment contribute to or are predictive of the increased prevalence of aneuploidy observed in oocytes (Battaglia *et al.*, 1996). Sanfins *et al.* (2003) reported differences in meiotic spindle structure and assembly during *in vitro* and *in vivo* maturation of mouse oocytes. Recently, Sakai *et al.* (2011) reported that oocyte fertility and developmental potency can be explained by the distance between the pericentriolar materials (PCM) of the spindle. The PCM distance is related to the developmental rate of embryos (Sakai *et al.*, 2011). With the recent, dramatic increase in the use of assisted reproductive therapy (ART), there is now a desire to develop non-invasive and convenient methods to predict oocyte and/or embryonic quality based on morphometric and morphological parameters of the MII spindle of maturing oocytes *in vivo* or *in vitro* (Coticchio *et al.*, 2013 **)**.

PBs are by-products of meiotic division in oocytes. The removal of the first and/or second PB is an indirect approach to infer the genetic or chromosomal status of oocytes (Montag *et al.*, 2013). Both PBs are not required for successful fertilization or normal embryonic development (Geraedts *et al.*, 2011; Christopikou *et al.*, 2013). PB biopsy is effective for the diagnosis of structural and numerical chromosomal aberrations in human oocytes using fluorescent *in situ* hybridization and array-CGH (Mailhes *et al.*, 1998; Montag *et al.*, 2004; Verlinsky *et al.*, 2005). Nevertheless, the use of PB biopsy and array-CGH for PGD is still a matter of debate, owing to the high incidence of postmeiotic aneuploidies that are undetectable by the PB approach (Capalbo *et al.*, 2013). Zhou *et al.* (2015) did not observe significant differences in the pregnancy or implantation rates with respect to PB morphology, and PB-based aneuploidy screening is poorly predictive of embryo ploidy and the reproductive potential of PBs (Salvaggio *et al.*, 2014); accordingly, controversy still exists. These findings suggest that a PB analysis combined with meiotic spindle images are useful as a new index to sort transplant embryos and predict oocyte fertility and developmental potential for PDG.

The objective of this study was to classify spindle and PB1 chromosomal images of ovulated oocytes at various time points until over-maturation to predict the developmental potency of MII oocytes in mice.

Materials and methods

Animals and oocyte collection

The study protocol followed the laboratory animal care guidelines, and all procedures were conducted in accordance with the guidelines of the Ethics Committee for the Care and Use of Laboratory Animals for Research of Niigata University, Japan.

DBA/2 male mice and C57BL6 female mice were purchased from the Charles River Laboratories Japan, Inc. (Yokohama, Japan), and B6D2F1 mice were bred in our laboratory. B6D2F1 male and female mice that were at least 8 weeks old were used for all experiments.

To obtain oocytes, mice were primed with 5 IU of pregnant mare's serum gonadotropin (PMSG) (Calbiochem, La Jolla, CA, USA) and then with 5 IU of human chorionic gonadotropin (hCG) (Calbiochem) after 48 h. At 12, 15, 20, and 25 h after hCG treatment, cumulus–oocyte complexes (COCs) released from oviductal ampullae were collected in 100-μL droplets of Chatot-Ziomek-Bavister (CZB) medium containing bovine serum albumin (BSA). The cumulus cells were removed by treatment with 1% hyaluronidase at room temperature. Cumulus-free oocytes were collected in CZB-BSA medium. The collected oocytes were either used to stain the spindle and PB1 or inseminated *in vitro* and cultured. Collected oocytes were either used to stain the spindle and PB1 ($n = 21$) or inseminated *in vitro* and cultured ($n = 19$).

Fixation of oocytes and immunofluorescence staining

Immunolocalization in oocytes was examined according to the methods described in Sakai *et al.* (2011). Briefly, oocytes were washed four times in phosphate-buffered saline (PBS) containing 0.1% polyvinyl alcohol (PVA; PBS-PVA), and denuded oocytes were fixed with 2% paraformaldehyde (Sigma, St. Louis, MO, USA) in PBS–PVA at room temperature for 40–60 min. Oocytes were washed four times in PBS–PVA and stored at 4°C overnight in PBS–PVA–BSA. Microtubules were detected using anti-α-tubulin (Sigma; 1:500) at room temperature for 40 min and Alexa Fluor 488-labelled anti-mouse IgG antibodies (Molecular Probes, Eugene, OR, USA; 1:500) at room temperature for 30 min. Oocytes were washed four times in PBS–PVA–BSA. They were permeabilized in 2.5% Tween 20 (BioRad, Hercules, CA, USA) at room temperature and were washed four times in PBS–PVA–BSA. The chromosomes were stained with 2.5 μl of 4′,6-diamidino-2-phenylindole (DAPI; Invitrogen, Carlsbad, CA, USA), and oocytes were viewed using a fluorescence microscope (BX60; Olympus, Tokyo, Japan).

https://doi.org/10.1017/S096719941600023X Published online by Cambridge University Press

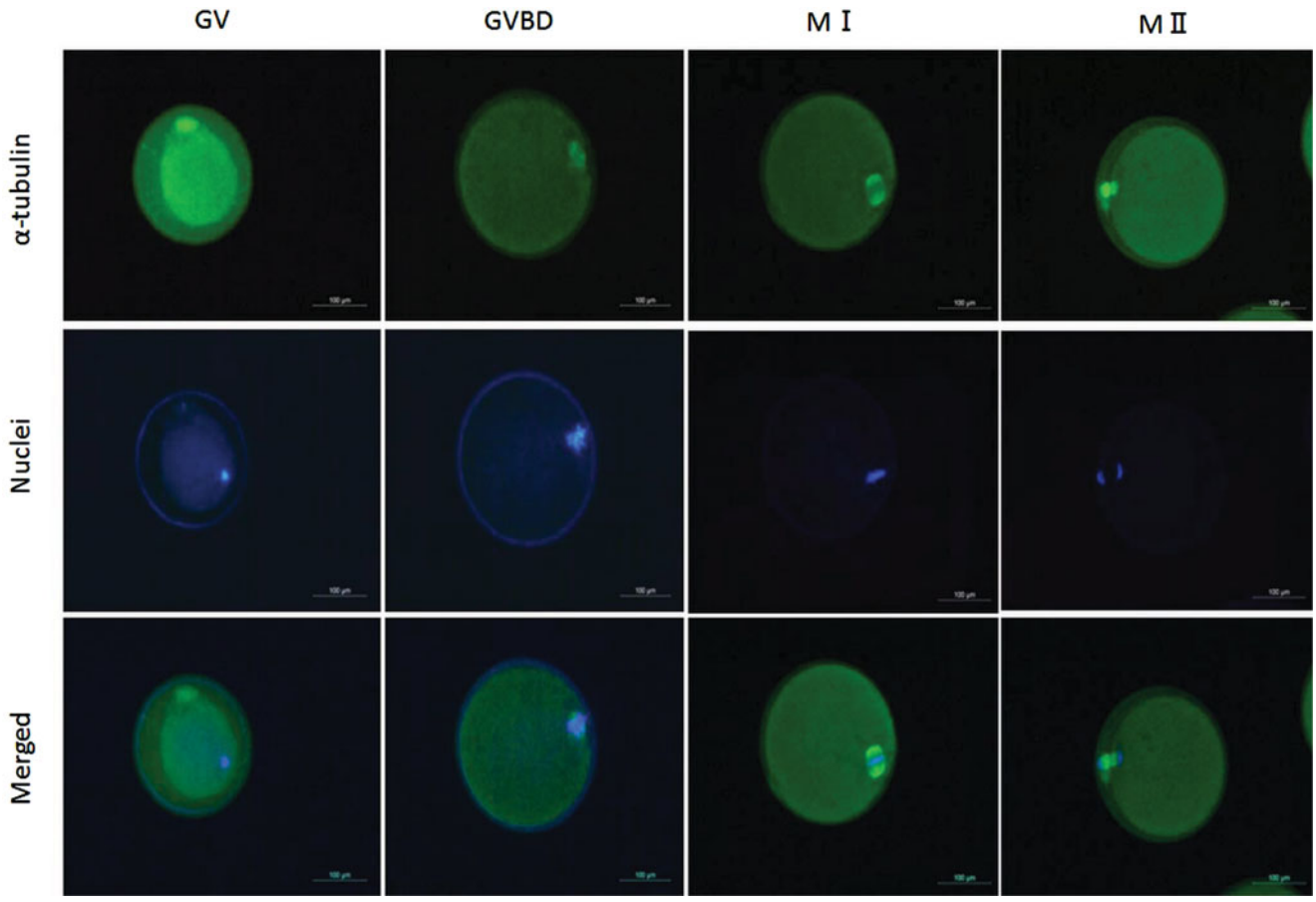

Figure 1 Representative images of oocyte spindles and first polar body chromosomes of immature oocytes. Immature oocytes of the germinal vesicle (GV), germinal vesicle breakdown (GVBD), metaphase I (MI), anaphase I (AI), telophase I (TI), and metaphase II (MII) stages were stained with α-tubulin (green) and nuclei were stained blue. Magnification ×200. Scale bar = 100 μm.

In vitro fertilization and embryo culture

Sperm were collected from both caudae epididymides and pre-incubated for 1–2 h in 100 μL of human tubal fluid medium, to allow capacitation before insemination in a humidified atmosphere at 5% CO_2 in air and 37°C. After incubation, the 10 μL sperm suspension was added to 90 μL droplets of the *in vitro* fertilization (IVF) human tubal fluid medium at a final concentration of 1–5 × 10^6 sperm/mL. After 6 h, the inseminated oocytes were washed thoroughly five times and then cultured in potassium simplex optimized medium until the blastocyst stage in an incubator. Fertilization rates were calculated as the total number of 2-cell embryos divided by total number of inseminated oocytes multiplied by 100.

Statistical analysis

All data are expressed as mean ± standard deviation (SD). The data were subjected to a one-way analysis of variance (ANOVA) and Fisher's protected least significant difference *post-hoc* test implemented in STATVIEW (Abacus Concepts Inc., Berkeley, CA, USA). *P*-values of less than 0.05 indicated statistical significance. All the correlation coefficient were obtained using simple regression analysis (Excel software).

Results

Classification of spindle and first polar body chromosome images in immature oocytes

The spindle and PB1 chromosome images after immunostaining were categorized during the maturation of oocytes. Representative images of oocyte spindles and PB1 are shown in Fig. 1. The percentage of oocytes in each stage, including the germinal vesicle, germinal vesicle breakdown, MI, and AI–telophase I (TI) stages, are shown in Table 1. When oocytes were collected at 12, 15, 20, and 25 h

https://doi.org/10.1017/S096719941600023X Published online by Cambridge University Press

Table 1 Percentages of oocytes in each stage based on spindle and first polar body chromosome images

Treatment	Number of oocytes (*N*)	GV (germinal vesicle) (%)	GVBD (%)	MI (%)	AI–TI (%)	MII∗ (%)	Fragmentation (%)	Others (%)
12 h	103 (5)	6 (6)^{a}	10 (10)^{a}	37 (36)^{a,b}	4 (4)^{a}	27 (25)^{a}	19 (19)	0 (0)
15 h	97 (4)	2 (2)^{a}	11 (11)^{a}	36 (37)^{a}	8 (8)^{a}	22 (23)^{a}	14 (14)	4 (4)
20 h	81 (4)	2 (3)^{a}	7 (9)^{a}	12 (15)^{b,c}	0 (0)^{a}	50 (62)^{b}	10 (13)	0 (0)
25 h	118 (4)	0 (0)^{a}	0 (0)^{a}	4 (3)^{c}	1 (0)^{a}	104 (88)^{b}	5 (4)	4 (3)

$^{a–c}$Values with different superscripts within each column are significantly different ($P < 0.05$).
∗MII includes postovulatory oocytes.
GV, germinal vesicle; GVBD, germinal vesicle breakdown; *N*, number of female mice.

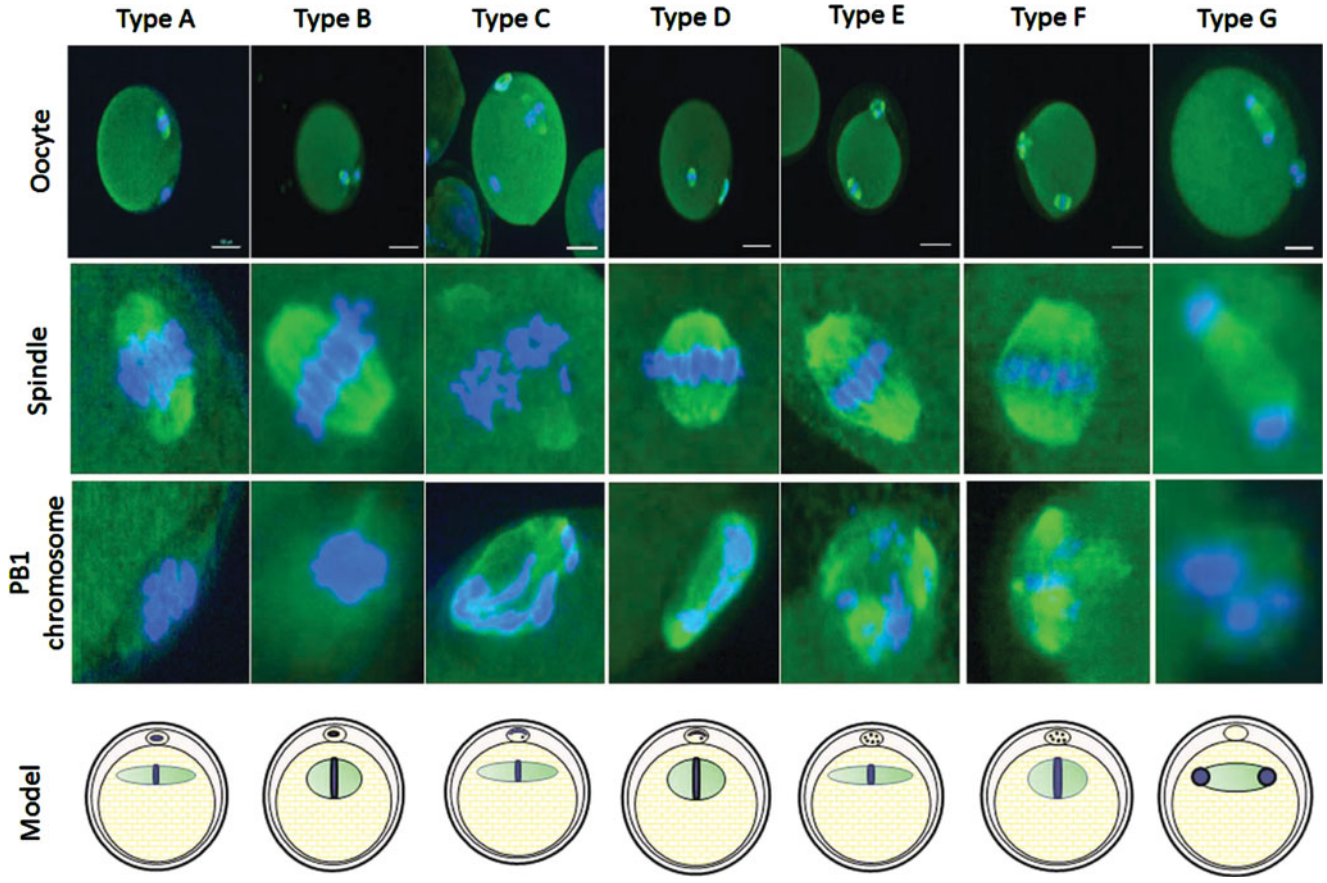

Figure 2 Classification of spindle and first polar body chromosome images in MII oocytes. Type A, spindle (tapered) and PB1 chromosome (aggregated); Type B, spindle (barrelled) and PB1 chromosome (aggregated); Type C, spindle (tapered) and PB1 chromosome (separated); Type D, spindle (barrelled) and PB1 chromosome (separated); Type E, spindle (tapered) and PB1 chromosome (dot); Type F, spindle (barrelled) and PB1 chromosome (dot); Type G, spindle (collapsed) and PB1 chromosome (collapsed). Magnification ×200. Scale bar = 100 μm.

after hCG injection, the MI rates were 36, 37, 15 and 3%, respectively. The MI rate was significantly lower ($P < 0.05$) for oocytes collected at 12 and 15 h after hCG injection than at 25 h after hCG injection. MII oocytes represented approximately 25% of the total number of oocytes collected in the 12-h and 15-h treatments, and these rates were significantly different ($P < 0.05$) than those observed in the 20 h and 25 h treatments.

Classification of spindle and first polar body chromosome images in MII oocytes

To determine whether time influenced the spindle and PB1 chromosome images, we collected oocytes at various time points after hCG injection. We categorized the spindle and PB1 chromosome images as Type A through G (Fig. 2). The percentages of spindles in the MII oocyte images belonging to each class are shown

https://doi.org/10.1017/S096719941600023X Published online by Cambridge University Press

Table 2 Classification of MII oocytes based on spindle images

Treatment	Number of oocytes (*n*)	Tapered (%)	Barrelled (%)	Collapsed (%)	Other (%)
12 h	27 (5)	5 (19)^{a}	21 (78)^{a}	0 (0)^{a}	1 (4)
15 h	22 (4)	10 (45)^{b}	10 (45)^{b}	2 (9)^{a}	0 (0)
20 h	50 (4)	4 (8)^{c}	8 (16)^{c}	33 (66)^{b}	5 (10)
25 h	104 (4)	3 (3)^{c}	2 (2)^{c}	89 (86)^{b}	10 (10)

$^{a–c}$Values with different superscripts within each column are significantly different ($P < 0.05$).
n, number of female mice.

Table 3 Classification of MII oocytes based on first polar body chromosome images

Treatment	Number of oocytes (*n*)	Aggregated (%)	Separated (%)	Dot (%)	Collapsed (%)	Other (%)
12 h	27 (5)	16 (59)^{a}	6 (22)^{a,b}	4 (15)^{a}	0 (0)^{a}	1 (4)
15 h	22 (4)	4 (18)^{a,b}	14 (64)^{a}	2 (9)^{a}	2 (9)^{a}	0 (0)
20 h	50 (4)	3 (6)^{b}	5 (10)^{a,b}	4 (8)^{a}	33 (66)^{b}	5 (10)
25 h	104 (4)	2 (2)^{b}	3 (3)^{b,c}	0 (0)^{a}	89 (86)^{b}	10 (10)

$^{a–c}$Values with different superscripts within each column are significantly different ($P < 0.05$).
n, number of female mice.

Table 4 Number of MII oocytes combined with spindle and first polar body chromosome images

Treatment	Number of oocytes (*n*)	Type A (%)	Type B (%)	Type C (%)	Type D (%)	Type E (%)	Type F (%)	Type G (%)	Other (%)
12 h	27 (5)	2 (7.4)^{a}	14 (51.8)^{a}	1 (3.7)^{a}	5 (18.5)^{a}	2 (7.4)^{a}	2 (7.4)^{a}	0 (0.0)^{a}	1 (3.7)
15 h	22 (4)	0 (0.0)^{a}	4 (18.2)^{b}	9 (40.9)^{b}	5 (22.7)^{a}	1 (4.5)^{a}	1 (4.5)^{a}	2 (9.1)^{a}	0 (0.0)
20 h	50 (4)	1 (0.2)^{a}	2 (0.4)^{b}	1 (0.2)^{a}	4 (0.8)^{b}	2 (0.4)^{a}	2 (0.4)^{a}	33 (66.0)^{b}	5 (1.0)
25 h	104 (4)	0 (0.0)^{a}	2 (1.9)^{b}	3 (2.9)^{a}	0 (0.0)^{b}	0 (0.0)^{a}	0 (0.0)^{a}	89 (85.6)^{c}	10 (9.6)

Type A, spindle (tapered) and PB1 chromosome (aggregated); Type B, spindle (barrelled) and PB1 chromosome (aggregated); Type C, spindle (tapered) and PB1 chromosome (separated); Type D, spindle (barrelled) and PB1 chromosome (separated); Type E, spindle (tapered) and PB1 chromosome (dot); Type F, spindle (barrelled) and PB1 chromosome (dot); Type G, spindle (collapsed) and PB1 chromosome (collapsed). $^{a-c}$Values with different superscripts within each column are significantly different ($P < 0.05$).
n, number of female mice.

in Table 2. The frequency of oocytes with tapering-type spindles was significantly ($P < 0.05$) different between 15 h and other time points. The frequencies of barrel-type spindles were 78% at 12 h, 45% at 15 h, 16% at 20 h, and 2% at 25 h, and there were significant differences ($P < 0.05$) between 12 and 15 h, 12 and 20 h, 12 and 25 h, 15 and 20 h, and 15 and 25 h. The frequency of barrel-type MII oocytes was significantly higher ($P < 0.05$) when oocytes were collected at 12 h after hCG injection than at other time points. The rate of MII oocytes that exhibited the collapsed spindle type was 0% at 12 h, 9% at 15 h, 66% at 20 h, 86% at 25 h, and significant differences ($P < 0.05$) were detected between oocytes at 12–15 h and 20–25 h.

The classification of PB1 chromosome images in MII oocytes is summarized in Table 3. The frequencies of aggregate-type PB1 in MII oocytes were 59% at 12 h, 18% at 15 h, 6% at 20 h, and 2% at 25 h, and there were significant differences ($P < 0.05$) between oocytes at 12 and 20 h and at 12 and 25 h. When oocytes were collected at 12, 15, 20, and 25 h after hCG injection, the observed frequencies of separation-type PB1 were 22%, 64%, 10%, 20%, and 3%, and a significant difference ($P < 0.05$) was observed between 15 and 25 h after hCG injection. Dot-type PB1 MII oocytes did not differ significantly among treatments. At 20 and 25 h after hCG treatment, collapsed-type PB1 was significantly ($P < 0.05$) more frequent than at 12 and 15 h after hCG treatment.

We combined spindle and PB1 chromosome images from each treatment group (Table 4). Barrel-type spindles and aggregate-type PB1 (Type B) were the major types observed at 12 h after hCG injection. When oocytes were collected 15 h after injection, spindles and

https://doi.org/10.1017/S096719941600023X Published online by Cambridge University Press

Table 5 Developmental potency of oocytes by IVF at various time points after hCG injection

Treatment	Number of oocytes (*n*)	2-cell (%)	Morula (%)	Blastocyst (%)
12 h	119 (6)	74 (62)[a]	65 (55)[a]	73 (61)[a]
15 h	179 (5)	91 (51)[a,b]	90(50)[a]	83 (46)[a]
20 h	102 (4)	21 (21)[a,b]	45 (44)[a,b]	43 (42)[a]
25 h	107 (4)	23 (21)[b]	16 (15)[b]	10 (9)[b]

[a,b]Values with different superscripts within each column are significantly different ($P < 0.05$).
n, number of female mice.

PB1 chromosomes were tapered and separated (Type C), respectively. At 20 and 25 h after treatment, spindle and PB1 images were collapsed into G-type.

Differences in spindle and PB1 morphologies among MII oocytes influence fertilization and developmental potency

To determine whether the observed differences in spindle and PB1 images in MII oocytes are associated with fertilization, we performed IVF at various time points after hCG injection. As shown in Table 5, the rate of development to 2-cell embryos did not differ between the 12-h and 15-h treatments. There was a significant decrease ($P < 0.05$) in the frequency of 2-cell embryos between the 12- and 25-h treatments. The rates of development to the blastocyst stage at 12, 15, 20, and 25 h post-hCG injection were 61, 46, 42 and 9%, respectively. Moreover, significant differences ($P < 0.05$) were observed between 12 and 25 h, 15 and 25 h, and 20 and 25 h.

Correlations between spindle or PB1 type frequencies and developmental potency are shown in Figure 3. The developmental potency of MII oocytes was correlated with the rates of barrel-type spindles ($R^2 = 0.9$), aggregate-type PB1 ($R^2 = 0.8$), and dot-type PB1 ($R^2 = 0.8$).

Discussion

It is important to identify reliable indicators of oocyte quality for efficient embryo production and successful infertility treatment. We classified spindle and PB1 chromosome images in ovulated oocytes over time until postovulation to predict the developmental potency of MII oocytes in mice.

When we collected oocytes and stained the spindles and PB1 chromosomes at 12 and 15 h after hCG injection, the frequencies of MII-maturated oocytes were significantly lower than those of oocytes collected at 20 and 25 h after hCG injection. However, the rate of development to the blastocyst stage was highest at 12 h after hCG treatment than at other time points, regardless of the approximately 40% of oocytes in MI. This result indicated that MI oocytes matured spontaneously *in vitro* in a 6-h period during the IVF process. It is possible that the fertilization ability and the developmental potency of oocytes were high immediately after the first meiotic division was completed, i.e. just after the first polar body was produced at the MII stage. Hence, even for oocytes at 25 h post-hCG treatment, in which the chromosomes were over-matured after IVF, the rate of development to the blastocyst stage was low. These results indicate that oocytes collected at 12–25 h after hCG injection have a distinct rate of development to the blastocyst stage; accordingly, it is possible to estimate and evaluate oocyte or embryonic potency using spindle and/or first polar body chromosome images.

To determine whether time influenced spindle images after hCG injection, we categorized spindles as being tapering- or barrel-type. Our results showed that the frequency of barrel-type spindles was significantly higher in the 12-h hCG treatment of MII oocytes than in other treatments. This indicates that barrel-type spindles have high potential to develop to blastocysts after IVF. Furthermore, the percentage of tapered spindles was low at 12 h; however, it increased at 15 h (from 19 to 45%), suggesting that during culture, oocyte spindle shape changed from barrelled to tapered, and they became more competent to reach the blastocyst stage. However, Sakai *et al.* (2011) suggested that *in vivo* matured oocytes with tapered-type spindles and *in vitro* matured oocytes with a barrel spindle have a high incidence of reaching the blastocyst stage based on experimental evaluations of developmental potency and fertility according to the distance between PCMs of spindles. In our experiment, when we collected oocytes at 15 h after hCG injection, nearly identical rates of barrel-type and tapering-type spindle images were observed, even if the tapering-type MII oocytes did not differ in the rate of development to the blastocyst stage. Therefore, it is necessary to develop methods to predict oocyte and/or embryonic quality based on the MII spindles

https://doi.org/10.1017/S096719941600023X Published online by Cambridge University Press

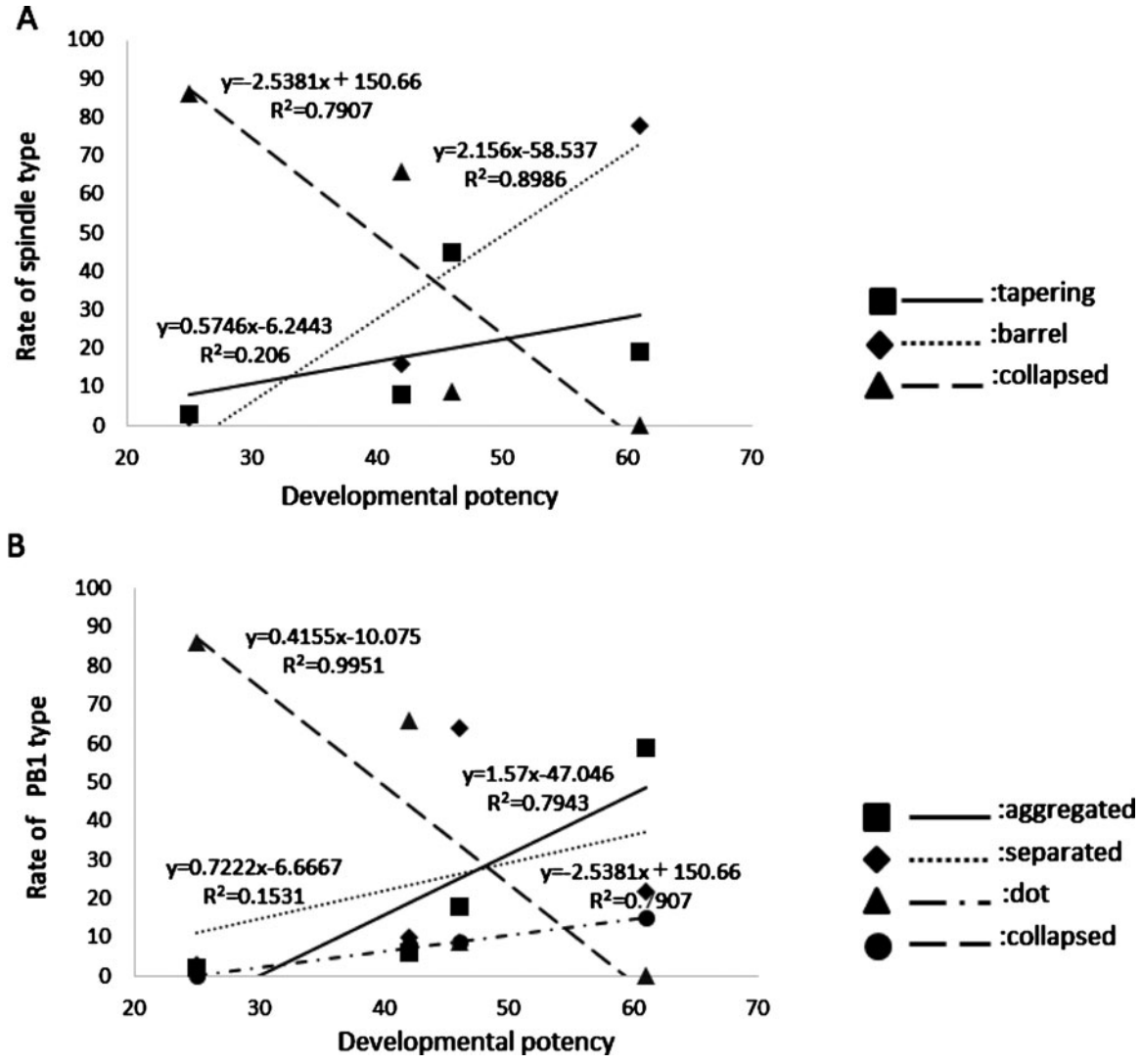

Figure 3 Correlation between the rate with frequency of spindle or PB1 type, and developmental potency. (*A*) Correlation between the rate with frequency of each spindle type and developmental potency. (*B*) Correlation between the rate with frequency of each PB1 type and developmental potency.

of oocytes or a combination between MII spindles and other indicators, such as PB1 images.

During maturation, oocytes eject half of their homologous chromosomes into PB1, which contains a redundant set of chromosomes plus a small amount of cytoplasmic organelles, and the extrusion of PB1 is an important hallmark of oocyte meiotic maturation (Fabritius *et al.*, 2011; Fabian *et al.*, 2012; Wei *et al.*, 2015). Polar body DNA shares remarkable homology with oocyte DNA; hence, an analysis of polar body DNA provides insight into oocyte genomes and telomeres, which may enhance the prediction of embryo developmental competence (Keefe *et al.*, 2015).

When we stained the PB1 chromosomes of MII oocytes at various collection times after hCG injection, they were classified as aggregate type, separation type or dot type. For the PB1 chromosomes collected at 12 h after hCG injection, the frequency of aggregate-type images was higher than those of images obtained at other time points, indicating that the aggregate-type PB1 chromosomes in MII oocytes have fertilization and developmental potency. For the PB1 chromosomes images collected at 15 h after hCG injection, the frequency of separation-type chromosomes was higher than it was at other time points. It is thought that the type of PB1 chromosome varies from aggregate type to dot type to separation type. In addition, when we evaluated MII oocytes based on PB1 images, the incidence of blastocyst development for aggregate-type chromosomes was the highest, but even separation-type, dot-type, or early over-maturational states developed to blastocysts. It is thought that more detailed information can be obtained by observing PB1 chromosome images of MII oocytes collected at

https://doi.org/10.1017/S096719941600023X Published online by Cambridge University Press

different times and evaluated with respect to developmental potency in individual fertilized oocytes. This finding is supported by Coticchio *et al.* (2013), who showed that spindle characteristics are associated with chromosome misalignment and different oocyte types reflect genuine biological conditions.

The rate of collapse of spindle oocytes differed significantly among treatments, and was particularly high for the 20- and 25-h treatments. Collapsed spindle oocytes are associated with an increased probability of disorder in fertilization. Unlike the oocytes, PB1 always undergoes degeneration, i.e., it is programmed to die, even when fertilization occurs. The decay of PB1 is usually complete by approximately 20 h after its extrusion (Ortiz *et al.*, 1983). Oocytes collected at 20 h after hCG injection exhibit a malfunction in the Ca^{2+} pump of the endoplasmic reticulum via a calcium oscillation abnormality after fertilization (Igarashi *et al.*, 1997). In addition, the frequency of premature centromere separation increases as the time to oocyte collection after hCG injection increases (Mailhes *et al.*, 1998). However, when we collected oocytes at 20 h after hCG injection, collapse-type spindle oocytes were observed; the incidence of blastocysts was 42%, and significant differences among treatments were not found. Based on these results, developmental potency does not decrease substantially in oocytes with early spindle collapse. However, when we collected oocytes at 25 h after hCG injection, the incidence of blastocysts was 9%, and was significantly decreased. Based on examinations of the relationship between oocyte aging and delayed fertilization, it is well known that the IVF rate decreases as time increases. Additional studies about the time to oocyte collection after hCG injection and associated decreases in IVF incidence are necessary.

In conclusion, we found that the spindle shape changed from barrel-type to tapered-type during maturation, and PB1 chromosomes varied from aggregate- and dot-type to separation-type. The incidence of blastocyst development for aggregate-type chromosomes was the highest, but even separation-type, dot-type, or early over-maturational states developed to blastocysts. MII oocytes with barrel-type spindles and aggregate-type PB1 had high rates of fertilization and blastocyst development, and there were correlations between spindle and PB1 characteristics and the outcomes of IVF and embryo culture. However, the same oocyte cannot be stained and then fertilized *in vitro.* This approach can be predictive, i.e., the collection and fertilization times can be optimized for a population of oocytes; however, it cannot be applied to determine the developmental potential of a specific oocyte (as is done for PGD, where a blastomere is removed and analysed and a blastocyst can be then implanted). Images of spindles combined with those of PB1 enable the evaluation and prediction of oocyte and/or embryonic quality. Further studies should be conducted to determine the relationships between PB1 classification and foetal development using PB1 biopsy.

Acknowledgements

The authors are grateful to Dr Yumi Hoshino, Tohoku University, Japan, for providing technical advice on the immunofluorescence staining experiments. This work was supported by the Japan Society for the Promotion of Science.

Conflict of interest statement

The authors declare no competing financial interests.

References

Battaglia, D.E., Goodwin, P., Klein, N.A. & Soules, M.R. (1996). Influence of maternal age on meiotic spindle assembly in oocytes from naturally cycling women. *Hum. Reprod.* **11**, 2217–22.

Capalbo, A., Bono, S., Spizzichino, L., Biricik, A., Baldi, M., Colamaria, S., Ubaldi, F.M., Rienzi, L. & Fiorentino, F. (2013). Sequential comprehensive chromosome analysis on polar bodies, blastomeres and trophoblast: insight into female meiotic errors and chromosomal segregation in the preimplantation window of embryo development. *Hum. Reprod.* **28**, 509–18.

Christopikou, D., Tsorva, E., Economou, K., Shelley, P., Davies, S., Mastrominas, M. & Handyside, A.H. (2013). Polar body analysis by array comparative genomic hybridization accurately predicts aneuploidies of maternal meiotic origin in cleavage stage embryos of women of advanced maternal age. *Hum. Reprod.* **28**, 1426–34.

Coticchio, G., Guglielmo, M.C., Dal Canto, M., Fadini, R., Mignini Renzini, M., De Ponti, E., Brambillasca, F. & Albertini, D.F. (2013). Mechanistic foundations of the metaphase II spindle of human oocytes matured *in vivo* and *in vitro*. *Hum. Reprod.* **28**, 3271–82.

Fabian, D., Cikos, S., Rehak, P. & Koppel, J. (2012). Do embryonic polar bodies commit suicide? *Zygote* **22**, 10–7.

Fabritius, A.S., Ellefson, M.L. & McNally, F.J. (2011). Nuclear and spindle positioning during oocyte meiosis. *Curr. Opin. Cell. Biol.* **23**, 78–84.

Geraedts, J., Montag, M., Magli, M.C., Repping, S., Handyside, A., Staessen, C., Harper, J., Schmutzler, A., Collins, J., Goossens, V., van der Ven, H., Vesela, K. & Gianaroli, L. (2011). Polar body array CGH for prediction of the status of the corresponding oocyte. Part I: clinical results. *Hum. Reprod.* **26**, 3173–80.

Igarashi, H., Takahashi, E., Hiroi, M. & Doi, K. (1997). Aging-related changes in calcium oscillations in fertilized mouse oocytes. *Mol. Reprod. Dev.* **48**, 383–90.

https://doi.org/10.1017/S096719941600023X Published online by Cambridge University Press

Keefe, D., Kumar, M. & Kalmbach, K. (2015). Oocyte competency is the key to embryo potential. *Fertil. Steril.* **103**, 317–22.

Mailhes, J.B., Young, D. & London, S.N. (1998). Postovulatory ageing of mouse oocytes *in vivo* and premature centromere separation and aneuploidy. *Biol. Reprod.* **58**, 1206–10.

Montag, M., Van der Ven, K., Dorn, C. & Van der Ven, H. (2004). Outcome of laser-assisted polar body biopsy. *Reprod. Biomed. Online* **9**, 425–9.

Montag, M., Koster, M., Strowitzki, T. & Toth, B. (2013). Polar body biopsy. *Fertil. Steril.* **100**, 603–7.

Ortiz, M., Lucero, P. & Coxatto, H. (1983). Post ovulatory aging of human ova: spontaneous division of the first polar body. *Gamete Res.* **7**, 269–76.

Sakai, C., Hoshino, Y., Sato, Y. & Sato, E. (2011). Evaluation of maturation competence of metaphase II oocytes in mice based on the distance between pericentriolar materials of meiotic spindle: distance of PCM during oocyte maturation. *J. Assist. Reprod. Genet.* **28**, 157–66.

Salvaggio, C.N., Forman, E.J., Garnsey, H.M., Treff, N.R. & Scott, R.T. Jr. (2014). Polar body based aneuploidy screening is poorly predictive of embryo ploidy and reproductive potential. *J. Assist. Reprod. Genet.* **31**, 1221–6.

Sanfins, A., Lee, G.Y., Plancha, C.E., Overstrom, E.W. & Albertini, D.F. (2003). Distinctions in meiotic spindle structure and assembly during *in vitro* and *in vivo* maturation of mouse oocytes. *Biol. Reprod.* **69**, 2059–67.

Stern, H.J. (2014). Preimplantation genetic diagnosis: Prenatal testing for embryos finally achieving its potential. *J. Clin. Med.* **3**, 280–309.

Uchiyama, K., Kikuchi, M., Ieda, S., Yamashita, N., Takehara, Y., Kaijima, H. & Kato, O. (2008). Efficiency of oocyte spindle observation with a LC-Polscope. *J. Mamm. Ova Res.* **25**, 105–10.

Verlinsky, Y., Tur-Kaspa, I., Cieslak, J., Bernal, A., Morris, R., Taranissi, M., Kaplan, B. & Kuliev, A. (2005). Preimplantation testing for chromosomal disorders improves reproductive outcome of poor-prognosis patients. *Reprod. Biomed. Online* **11**, 219–25.

Wei, Y., Zhang, T., Wang, Y.P., Schatten, H. & Sun, Q.Y. (2015). Polar bodies in assisted reproductive technology: current progress and future perspectives. *Biol. Reprod.* **92**, 1–8.

Zhou, W., Fu, L., Sha, W., Chu, D. & Li, Y. (2015). Relationship of polar bodies morphology to embryo quality and pregnancy outcome. *Zygote* **22**, 1–7.